JOURNAL OF THERMOPHYSICS AND HEAT TRANSFER
Vol. 14, No. 2, April–June 2000

Investigations on Transient and Steady-State Performance of a Micro Heat Pipe

C. B. Sobhan,* Huang Xiaoyang,† and Liu Chang Yu‡
Nanyang Technological University, Singapore 639798, Republic of Singapore

A numerical study is presented of the vapor and liquid flow in a micro heat pipe with triangular channels, utilizing water as the working medium. The governing equations are derived taking into account the variation in the flow cross-sectional areas of the vapor and liquid phases and incorporating the phase change during the process. The velocity, pressure, and temperature distributions in the vapor and liquid, in the transient and steady states, are obtained from the analysis. The effective thermal conductivity of the micro heat pipe is calculated, and its dependence on the heat input and the heat transfer coefficient at the condenser section is investigated. The results of the analysis are compared with those available in literature and discussed in the light of the assumptions made and the extensions incorporated in the present model.

Nomenclature

A_c = area of cross section of the heat-pipe channel, m^2
C_l = specific heat of the liquid, J/kg K
C_v = specific heat at constant volume of the vapor, J/kg K
D_H = hydraulic mean diameter of the channel, m
d = one side of the triangular channel, m
E_l = total energy of the liquid per unit volume, $\rho_l(C_l T + \frac{1}{2}u_l^2)$, J/m^3
E_v = total energy of the vapor per unit volume, $\rho_v(C_v T + \frac{1}{2}u_v^2)$, J/m^3
f = friction coefficient
h_{fg} = latent heat of vaporization, J/kg
h_0 = heat transfer coefficient at the condenser, W/m^2 K
k = thermal conductivity, W/mK
k_{copper} = thermal conductivity of copper, W/mK
k_{eff} = effective thermal conductivity of the heat pipe, W/mK
k^* = thermal conductivity ratio, $k_{\text{eff}}/k_{\text{copper}}$
L = length of the heat pipe, m
P = pressure, Pa
P_{sat} = saturation pressure, Pa
Q_{in} = heat input at the evaporator, W
Q_0 = heat dissipation at the condenser, W
q = heat flux, W/m^2
R = gas constant, J/kg K
r = radius of curvature of the meniscus, m
r_0 = initial radius of curvature of the meniscus, m
T = temperature, K
T_{amb} = ambient temperature, K
t = time, s
u = axial velocity, m/s
V_{il} = interfacial liquid velocity, m/s
V_{iv} = interfacial vapor velocity, m/s
x = axial coordinate
$\beta_i, \beta_l, \beta_{\text{lw}}$ = geometric area coefficients (Appendix)
ΔT = temperature difference, $T - T_{\text{amb}}$, K
μ = viscosity, N s/m^2
ρ = density, kg/m^3
σ = surface tension, N/m

Subscripts

amb = ambient
c = condenser
e = evaporator
i = interface
l = liquid
li = liquid interface
lw = liquid wall
v = vapor
vi = vapor interface
vw = vapor wall

Received 1 March 1999; revision received 17 December 1999; accepted for publication 3 January 2000.

*Postdoctoral Research Fellow, School of Mechanical and Production Engineering, Nanyang Avenue; currently Visiting Scholar, Cooling Technologies Research Consortium, School of Mechanical Engineering, Purdue University, West Lafayette, IN 47907; permanent address: Senior Lecturer, Department of Mechanical Engineering, Regional Engineering College, Calicut 673 601, India.
†Associate Professor, School of Mechanical and Production Engineering, Nanyang Avenue.
‡Professor, School of Mechanical and Production Engineering, Nanyang Avenue.

Introduction

THERMAL control is a crucial aspect in ensuring reliable performance of microelectronic devices. Heat dissipation from such devices is an important problem, with the high levels of heat flux intensities encountered in miniature components, leading to a high surface temperature. It is required to keep the devices at optimum operating temperatures by dissipating the heat generated in them. The extent to which this can be accomplished by conventional heat sinks is limited, requiring novel techniques. An interesting alternative method is to make use of the latent heat transfer associated with the phase change of a working fluid in a closed circulation device such as the micro heat pipe that can be attached directly to the electronic chip.

The construction and operation of the micro heat pipe have some essential differences from those of the conventional heat pipe. In the conventional heat pipe, a wick structure is used either in the form of a mesh or as grooves, providing the wicking or capillary effect for the circulation of the liquid phase. The micro heat pipe consists of microchannels, defined as channels where the capillary radius is comparable with the hydraulic radius of flow. A single channel or an array of such channels can be used as a micro heat pipe, each channel serving as an individual heat transport device. The channels are of polygonal cross section, the corners of which provide the capillary action for flow of the liquid. Thus, under operation, the vapor fills the central portion of the microchannel, and the liquid flows back adjacent to the corners.

Experimental and analytical investigations on single trapezoidal micro-heat-pipe channels were conducted by Babin et al.[1] In the

analytical work, a steady-state, one-dimensional model imposed the extremely small characteristic dimensions of the micro-heat-pipe channel on the conventional-heat-pipe model, and the effects of these were examined. The analytical results were compared with the steady-state experimental results on copper and silver heat pipes. Ma and Peterson[2] presented analytical expressions for the minimum meniscus radius and maximum capillary heat transport limit in micro heat pipes, incorporating the shear stress at the interfaces, contact angle effects, vapor pressure drop, tilt angle, groove dimensions, and channel angle effects. Comparisons were made with experimental data from triangular grooves and micro heat pipes, to verify the expressions. A one-dimensional model of the evaporator and adiabatic sections of a micro heat pipe operating under steady-state conditions was developed by Longtin et al.[3] This model incorporated the interfacial and vapor shear stress and the convection and body force terms in the momentum equation, but assumed that the vapor temperature is constant throughout the length of the heat pipe, thus requiring solution of only the energy equation for the liquid phase. Numerical solutions were obtained for the pressure, velocity, and film thickness distributions along the length of the pipe. The analysis was restricted to the evaporator and adiabatic sections of the micro heat pipe. A transient numerical model capable of predicting the maximum heat transport capacity prior to dry out in a micro heat pipe was developed by Wu and Peterson.[4] The accuracy of this model has been verified by Wu et al.,[5] comparing it with the transient experimental results on tapered micro heat pipes specifically designed for use in the thermal control of ceramic chip carriers. It was found that the numerical model accurately predicts the steady-state behavior, but underestimates the transient response. Khrustalev and Faghri[6] developed a detailed mathematical model for the heat and mass transfer processes in micro heat pipes with polygonal cross section that describes the liquid distribution and thermal characteristics. The predicted results were compared with available experimental data. The importance of the liquid fill, the minimum wetting contact angle, and the shear stresses at the liquid–vapor interface in predicting the maximum heat transfer capacity and thermal resistance was discussed. Peterson and Ma[7] presented a mathematical model of the liquid friction factor for flow in triangular grooves, considering the interfacial shear stresses due to liquid–vapor frictional interactions for countercurrent flow. The governing liquid flow equations were solved, for cases where the liquid surface is strongly influenced by the vapor flow direction and velocity, to yield the velocity distribution for countercurrent liquid–vapor flow. Numerical solutions for channel angles of 20, 30, 40, and 60 deg were compared with the corresponding experimental data. Swanson and Peterson[8] presented a thermodynamic model of the vapor–liquid interface in micro heat pipes where the axial pressure and temperature differences and the changes in local interfacial curvature were considered. The analysis has been utilized to develop relationships useful in defining quantitative restrictions and requirements for the operation of micro heat pipes.

Experimental investigations to verify the micro-heat-pipe concept and to determine the potential advantages of constructing an array of micro heat pipes as an integral part of semiconductor devices have been reported by Peterson et al.[9] Temperature gradients and maximum localized temperatures in silicon wafers with integral micro-heat-pipe arrays were compared with those for a plain ungrooved silicon wafer. Increased effective thermal conductivity of approximately 25% was obtained for the wafer with the micro-heat-pipe array. Chen et al.[10] reported visualization experiments on glass micro heat pipes. They studied the variation of flow patterns and its dependence on charge and heat input and presented measured temperature distributions for various flow patterns. They also modeled the micro heat pipe employing the concept of two-phase flow in porous media. Experimental investigations on micro heat pipes have also been conducted by Zhou et al.[11] and Zhang et al.,[12] and results of external measurements reported. Advances in the development and testing of micro heat pipes fabricated as an integral part of semiconductor wafers have been discussed by Peterson.[13] A summary of the analytical and numerical techniques used to model and to predict the performance of integral micro heat pipes has also been presented. A comprehensive review of literature related to miniature and micro heat pipes and discussions on the various limits of operation of these heat pipes are presented by Cao et al.[14]

In the present work, numerical solutions are obtained for the transient and steady-state operation of a micro heat pipe that consists of an evaporator and a condenser section. The model does not assume a constant vapor temperature along the heat pipe and solves the energy equation along with the other governing equations to yield the transient and steady-state distributions of the temperature, pressure, and velocity. The influences of the heat input at the evaporator section and the convective heat transfer coefficient at the condenser section are investigated. The effective thermal conductivity of the heat pipe is calculated, and the influence of the parameters on the performance is studied. The results are compared with those reported in literature, and the similarities and differences are discussed.

Formulation

A flat micro heat pipe with a number of microchannels in an array is a compact heat dissipation device that can be effectively utilized to dissipate heat by attaching it to an electronic chip. Each individual channel in the array serves as an independent micro heat pipe. Figure 1a shows the overall dimensions of one such device. The micro-heat-pipe channels are of triangular cross section with 0.3-mm side as shown in Fig. 1b. The channels are formed by fabricating grooves on a copper plate of thickness 0.65 mm and covering them with another copper plate of thickness 0.35 mm, so that the overall thickness of the heat pipe is 1 mm, as shown in Fig. 1c. The flow and heat transfer in one channel is analyzed.

The micro heat pipe considered in the present study consists of the externally heated evaporator section and the condenser section subjected to convective cooling. The channel considered is part of a flat micro heat pipe with an array of 40 triangular channels. The maximum heat load capacity per channel in copper–water systems has been obtained by researchers,[5] and accordingly, heat load limited to a maximum of 0.25 W at the evaporator has been used in the present analysis. The system has been analyzed for various values of heat transfer coefficients at the condenser, assuming forced convection cooling by air, with a coolant temperature of 300 K. The transient analysis presented starts with an initial temperature of 300 K everywhere in the heat pipe and proceeds until steady state.

As the field variations in the channel are significant only in the axial direction due to the geometry, a one-dimensional model is expected to give fairly accurate results and is used in the present analysis. Analysis of micro heat pipes using one-dimensional models have been reported extensively in literature.[3,4] It is assumed that the thermophysical properties of the working fluid both in the liquid and vapor phases do not change significantly with temperature. The variation of the vapor density with temperature is incorporated in the calculation by interpolating from the available thermophysical property data.

The flow and heat transfer processes are governed by the continuity, momentum, and energy equations for the liquid and vapor phases. As phase change occurs, the local mass rates of flow of the two individual phases are connected through a mass balance at the interface between them. The areas of cross section of the vapor and liquid portions and the interfacial area vary along the length, due to progressive phase change as the fluids flow along the channel. The area variations are incorporated by suitable area coefficients, following the derivations presented in literature[3] (see Appendix). The local meniscus radius at the liquid–vapor interface to be used is calculated using the Laplace–Young equation, with a quasi-steady assumption. Refer to Fig. 1 for the configuration and the x direction used in the formulation and the Appendix for the area coefficients; the governing differential equations, after simplification, are written as follows.

1) Laplace–Young equation:

$$P_v - P_l = \sigma / r \tag{1}$$

2) Vapor phase, the continuity equation for the evaporator section:

$$\left(\frac{\sqrt{3}}{4} d^2 - \beta_l r^2 \right) \frac{\partial u_v}{\partial x} - 2\beta_l u_v r \frac{\partial r}{\partial x} + \beta_i \frac{\rho_l}{\rho_v} r V_{il} = 0 \tag{2}$$

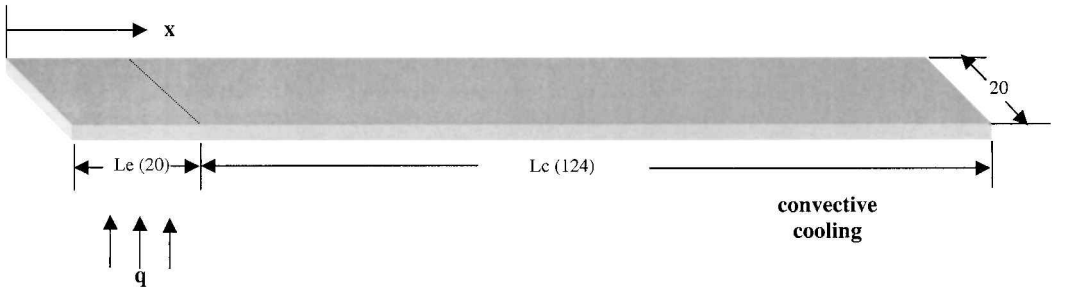

a) Arrangement of channels in the micro heat pipe

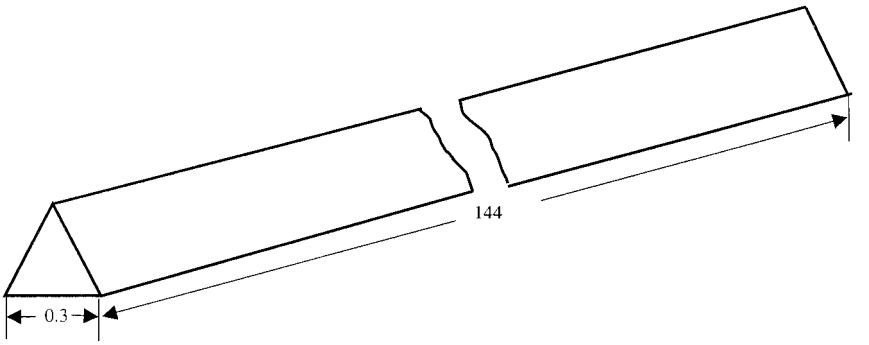

b) Channel under analysis

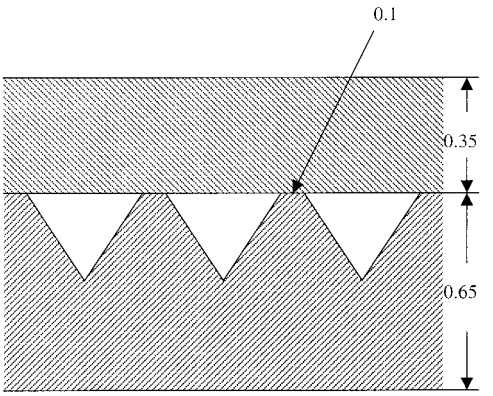

c) Cross-sectional view of the micro heat pipe showing channels and copper plates

Fig. 1 Schematic diagram showing the arrangement and details of the channels (dimensions in millimeters) in the microheat pipe.

and for the condenser section:

$$\left(\frac{\sqrt{3}}{4}d^2 - \beta_l r^2\right)\frac{\partial u_v}{\partial x} - 2\beta_l u_v r\frac{\partial r}{\partial x} - \beta_i\frac{\rho_l}{\rho_v}r V_{\text{il}} = 0 \qquad (3)$$

Note that the continuity equation for the vapor is written in terms of the liquid velocity, relating the liquid and vapor velocities at the interface using the mass balance. That is,

$$\rho_l V_{\text{il}} = \rho_v V_{\text{iv}} \qquad (4)$$

Vapor phase, momentum equation:

$$\rho_v\left(\frac{\sqrt{3}}{4}d^2 - \beta_l r^2\right)\frac{\partial u_v}{\partial t} = 2\rho_v\left(\frac{\sqrt{3}}{4}d^2 - \beta_l r^2\right)u_v\frac{\partial u_v}{\partial x}$$

$$- 2\rho_v\beta_l r u_v^2\frac{\partial r}{\partial x} + \left(\frac{\sqrt{3}}{4}d^2 - \beta_l r^2\right)\frac{\partial P_v}{\partial x}$$

$$+ \frac{1}{2}\rho_v u_v^2 f_{\text{vw}}(3d - \beta_{\text{lw}} r) + \frac{1}{2}\rho_v^2 u_v^2 f_{\text{vi}}\beta_l r \qquad (5)$$

Vapor phase, the energy equation for the evaporator section:

$$\left(\frac{\sqrt{3}}{4}d^2 - \beta_l r^2\right)\frac{\partial E_v}{\partial t} + \frac{\partial}{\partial x}\left[u_v\left(\frac{\sqrt{3}}{4}d^2 - \beta_l r^2\right)(E_v + P_v)\right]$$

$$= \frac{\partial}{\partial x}\left\{\frac{4}{3}\mu u_v\frac{\partial}{\partial x}\left[\left(\frac{\sqrt{3}}{4}d^2 - \beta_l r^2\right)u_v\right]\right.$$

$$\left. + k_v\frac{\partial}{\partial x}\left[\left(\frac{\sqrt{3}}{4}d^2 - \beta_l r^2\right)T_v\right]\right\} + q(3d - \beta_{\text{lw}} r) + h_{fg} V_{\text{il}}\rho_l\beta_l r$$

$$+ \frac{1}{2}\rho_v u_v^2 f_{\text{vw}} u_v(3d - \beta_{\text{lw}} r) + \frac{1}{2}\rho u_v^2 f_{\text{vi}} u_v\beta_i r \qquad (6)$$

and for the condenser section:

$$\left(\frac{\sqrt{3}}{4}d^2 - \beta_l r^2\right)\frac{\partial E_v}{\partial t} + \frac{\partial}{\partial x}\left[u_v\left(\frac{\sqrt{3}}{4}d^2 - \beta_l r^2\right)(E_v + P_v)\right]$$
$$= \frac{\partial}{\partial x}\left\{\frac{4}{3}\mu u_v \frac{\partial}{\partial x}\left[\left(\frac{\sqrt{3}}{4}d^2 - \beta_l r^2\right)u_v\right]\right.$$
$$\left. + k_v \frac{\partial}{\partial x}\left[\left(\frac{\sqrt{3}}{4}d^2 - \beta_l r^2\right)T_v\right]\right\} + h_{fg}V_{il}\rho_l\beta_l r$$
$$- h_0(3d - \beta_{lw}r)\Delta T + \frac{1}{2}\rho_v u_v^2 f_{vw}u_v(3d - \beta_{lw}r)$$
$$+ \frac{1}{2}\rho_v u_v^2 f_{vi}u_v\beta_i r \tag{7}$$

3) Liquid phase, the continuity equation for the evaporator section:

$$r\frac{\partial u_l}{\partial x} + 2u_l\frac{\partial r}{\partial x} - \frac{\beta_i}{\beta_l}V_{il} = 0 \tag{8}$$

and for the condenser section:

$$r\frac{\partial u_l}{\partial x} + 2u_l\frac{\partial r}{\partial x} + \frac{\beta_i}{\beta_l}V_{il} = 0 \tag{9}$$

Liquid phase momentum equation:

$$\rho_l r\frac{\partial u_l}{\partial t} = -2\rho_l\left(ru_l\frac{\partial u_l}{\partial x} + u_l^2\frac{\partial r}{\partial x}\right) - r\frac{\partial P_l}{\partial x}$$
$$+ \frac{1}{2}\rho_l u_l^2 f_{lw}\frac{\beta_{lw}}{\beta_l} + \frac{1}{2}\rho_l u_l^2 f_{li}\frac{\beta_i}{\beta_l} \tag{10}$$

Liquid phase, energy equation for the evaporator section:

$$\beta_l r^2\frac{\partial E_l}{\partial t} + \frac{\partial}{\partial x}\left[u_l\beta_l r^2(E_l + P_l)\right]$$
$$= \frac{\partial}{\partial x}\left[\frac{4}{3}\mu u_l\frac{\partial}{\partial x}(u_l\beta_l r^2) + k\frac{\partial}{\partial x}(\beta_l r^2 T_l)\right]$$
$$+ q\beta_{lw}r - h_{fg}V_{il}\rho_l\beta_i r + \frac{1}{2}\rho_l u_l^2 f_{lw}u_l\beta_{lw}r + \frac{1}{2}\rho_l u_l^2 f_{li}u_l\beta_i r \tag{11}$$

and for the condenser section:

$$\beta_l r^2\frac{\partial E_l}{\partial t} + \frac{\partial}{\partial x}\left[u_l\beta_l r^2(E_l + P_l)\right]$$
$$= \frac{\partial}{\partial x}\left[\frac{4}{3}\mu u_l\frac{\partial}{\partial x}(u_l\beta_l r^2) + k\frac{\partial}{\partial x}(\beta_l r^2 T_l)\right] + h_{fg}V_{il}\rho_l\beta_i r$$
$$- h_0\beta_{lw}r\Delta T + \frac{1}{2}\rho_l u_l^2 f_{lw}u_l\beta_{lw}r + \frac{1}{2}\rho_l u_l^2 f_{li}u_l\beta_i r \tag{12}$$

Thus, in the present work, a formulation using the continuity, momentum, and energy equations is utilized, and the field variations are obtained for both the evaporator and condenser regions of the heat pipe, proceeding on the lines suggested in literature.[3] The interfacial, liquid to wall, and vapor to wall friction coefficients utilized in the analysis were also calculated according to the discussions presented in literature.[3] These are calculated from the Reynolds number and the constant in the relation $f = k/Re$, where k depends on the geometry of the duct and accounts for the variation in geometry. The constant k is chosen as 13.3 for the liquid, assuming a triangular cross section and 14.7 for the geometry of the vapor channel varying from nearly triangular in the evaporator to almost circular where the interfaces meet.[3]

The vapor and liquid pressures are computed as follows. The equation of state is utilized for computing the pressure in the vapor. Because the vapor is either saturated or superheated, the ideal gas state equation is reasonably correct and is used extensively in heat pipe analysis.[15] For the liquid phase, as a first approximation, the Hagen–Poiseuielle equation is used, with the local hydraulic diameter for the wetted portion of the channel wall adjacent to the corners. The values of pressure are substituted back in the momentum equations and iterated for spatial convergence. The equations used are as follows.

Equation of state in the vapor:

$$P_v = \rho R_v T_v \tag{13}$$

The Hagen–Poiseuielle equation is used as a first approximation in the liquid:

$$\frac{\partial P_l}{\partial x} = -\frac{8\mu u_l}{(D_H^2/4)} \tag{14}$$

The boundary conditions at $x = 0$ and L are $u_l = 0$ and $u_v = 0$, and $\partial T/\partial x = 0$.

The initial conditions at $t = 0$, for all x are $P_v = P_l = P_{sat}$, $T_v = T_l = T_{amb}$, and $r = r_0$. At $x = 0$ and $t = 0$, then $P_l - P_v = \sigma/r_0$.

The value of r_0, the initial radius of curvature of the interface meniscus for the copper–water system, is adopted from literarture.[3] Detailed discussions on the selection of r_0 and the dependence of the solution on this are presented by Longtin et al.[3] In the present case also, as observed by them, it was found that the solution is unaffected by the initial selection of r_0 because in the subsequent steps the radius of curvature is calculated using the Laplace–Young equation.

Numerical Solution

The governing differential equations were solved using a finite difference scheme. In the finite difference formulation, central differences were used for second-order derivatives, and upwind differences were used for the convective terms. An explicit scheme is used with a time step size of 10^{-8} s, and stable, converged solutions were obtained by successive spatial grid refinement.

The steps involved in the solution procedure are summarized as follows.

1) Obtain the local meniscus radius from the Laplace–Young equation.

2) Obtain the interfacial vapor velocity from the vapor continuity equation and calculate the interfacial liquid velocity using the interface mass balance.

3) Use the vapor momentum equation to obtain the axial vapor velocity.

4) Obtain the vapor energy and vapor temperature from the vapor energy equation.

5) Calculate the vapor pressure using the equation of state for the vapor.

6) From the liquid continuity equation, obtain the liquid velocity derivative in terms of the interfacial liquid velocity obtained at step 2 and substitute into the liquid momentum equation.

7) Solve the liquid momentum equation to obtain the axial liquid velocity.

8) Obtain the liquid energy and temperature from the liquid energy equation.

9) Calculate the liquid pressure using Hagen–Poiseuille equation.

10) Substitute the liquid pressure back in the liquid momentum equation and iterate for spatial convergence.

11) The time stepping is continued until the system reaches steady state.

The primary results obtained from the calculation are the instantaneous local velocity, temperature, and pressure in the domain. Parametric studies were performed varying two input parameters, namely, the heat input at the evaporator and the convective heat transfer coefficient at the condenser, to study the dependence of the field variables on them. An effective thermal conductivity is defined for the heat pipe as follows, using an analogy with one-dimensional heat conduction in a solid rod:

$$k_{eff} = \frac{Q_{in}}{A_c[(T_e - T_c)/L]} \tag{15}$$

The effective thermal conductivity is normalized with respect to the thermal conductivity of copper as

$$k^* = k_{\text{eff}} / k_{\text{copper}} \tag{16}$$

The dependence of the effective thermal conductivity ratio at steady state, on the heat input at the evaporator was studied. The instantaneous effective thermal conductivity, using Q_0 in place of Q_{in} in Eq. (15) was also obtained, to study its transient variation.

Results and Discussion

Transient analysis of a micro heat pipe with triangular channels is performed in this study. The micro heat pipe analyzed utilizes water as the working medium and has evaporator and consenser sections. The transient period under analysis starts when the heat input is applied to the evaporator section with the heat pipe at the initial temperature of 300 K. The condenser section is cooled externally with an imposed heat transfer coefficient that is varied in the analysis, with a fixed coolant temperature of 300 K. Heat input values of 0.07, 0.11, 0.16, 0.2, and 0.25 W and heat transfer coefficients of 120, 130, and 150 W/m^2 K were used at the evaporator and condenser sections, respectively. The primary results of the analysis are the velocity, temperature, and pressure distributions in the vapor and the liquid. The effective thermal conductivity of the heat pipe was determined in all of the cases and normalized with the thermal conductivity of copper. The variations of the effective thermal conductivity ratio with respect to the input heat and the transient variations of the instantaneous effective thermal conductivity ratio were studied. Detailed discussions on the computational results are given.

Velocity Distribution

The distributions of the vapor and liquid velocities in a micro heat pipe are mostly determined by the following factors: 1) mass addition or depletion in the vapor and liquid streams and 2) the local variation of the cross-sectional areas of the vapor and liquid streams. In the present case, the micro heat pipe consists of only the evaporator and condenser sections. Figure 2 shows the local variation of the vapor velocity at various time instants and at steady state. The case presented is for an input power of 0.25 W to the channel and a convective heat transfer coefficient of 120 W/m^2 K at the surface of the condenser section; the nature of the variation is typical for all input power values and heat transfer coefficients used. The vapor velocity increases monotonically along the length of the evaporator section until its end. In the condenser section, it falls almost linearly. Even though there is a variation in the vapor flow area along the channel, this change is not significant enough to affect the linear velocity variation produced by the progressive mass addition and depletion processes due to the phase change at the evaporator and condenser sections. Similar variations are observed in the transient as well as steady states.

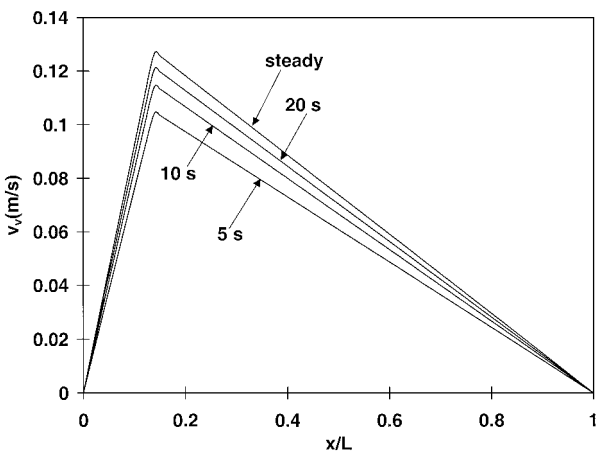

Fig. 2 Vapor velocity distribution along the channel at various time instants.

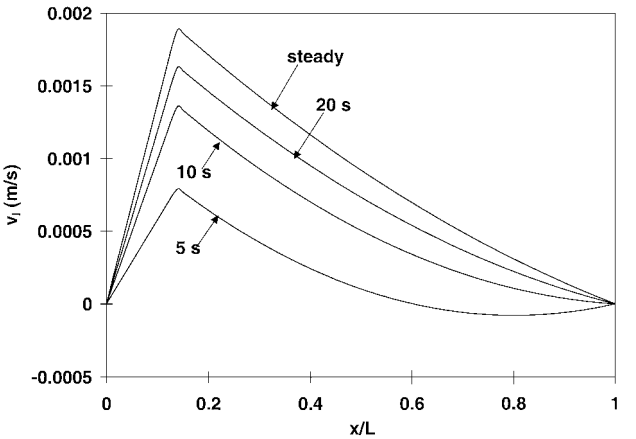

Fig. 3 Liquid velocity distribution along the channel at various time instants for the case presented in Fig. 2.

The distribution of the liquid velocity along the length of the heat pipe is shown in Fig. 3, for the same case as presented in Fig. 2. The velocities shown are in the negative x direction. The liquid velocity distributions show different trends in the condenser and the evaporator sections. The liquid formed at the condenser section flows to the evaporator section along the corners of the channel. In the early transient period, a flow reversal is noticed toward the condenser end. This is in accordance with the computational results presented previously in the literature.[4,5] The effect is due to the forcing of liquid from the evaporator region to the condenser region, as a result of lower evaporation rates at the early transient period. The phenomenon of flow reversal disappears when the process proceeds in time. In the evaporator section, the variation of the liquid velocity is a linearly decreasing one in the direction of flow. In the condenser section, the variation is not linear.

The deviation of the velocity profile from a linear one at the condenser section is attributed to the pronounced effect of the variation in the liquid cross-sectional area in this section. Because the liquid portion in the heat pipe is very small, this has a substantial effect in the flow velocity at the condenser section, where the area variation is maximum. However, at the evaporator section, the relatively smaller area variation does not produce any significant effect on the linear nature of the liquid velocity distribution that results due to the mass depletion.

Temperature Distribution

Efficient operation of a micro heat pipe is characterized by an almost uniform temperature along its length. This results in a high value of effective thermal conductance for the heat pipe. Temperature distributions in the vapor, along the heat pipe for three different conditions, are shown in Figs. 4–6. These are the distributions at various time instants for a typical case analyzed, steady-state distributions for different heat input values with the same convective heat transfer coefficient at the condenser, and the steady-state distributions for the same input power value at the evaporator with different heat transfer coefficients at the condenser. In all of the cases, it is found that the major drop in the vapor temperature takes place at the junction between the evaporator and condenser sections. A slight drop in temperature occurs along the evaporator, but except at the region near its beginning, in the condenser section, the temperature remains almost constant.

Figure 4 shows the transient variation of the vapor temperature distribution. In the initial transient period, the evaporator section where the input heat is applied heats up much faster, producing a larger drop of temperature across the sections. As the process continues, the vapor temperature drop becomes smaller, due to improved dissipation at the condenser, which in effect arrests the rate at which the evaporator temperature grows, and by the time the system reaches steady state, the drop becomes very small. In the case shown, with a heat input of 0.25 W at the evaporator, which is the maximum value used in the present study, and with a heat transfer coefficient

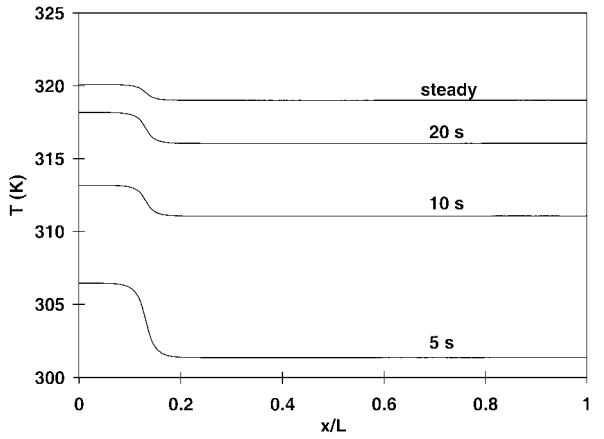

Fig. 4 Vapor temperature distribution along the length of the micro-heat-pipe channel, at various time instants, for a heat input of 0.25 W at the evaporator and a heat transfer coefficient of 120 W/m^2 K at the condenser.

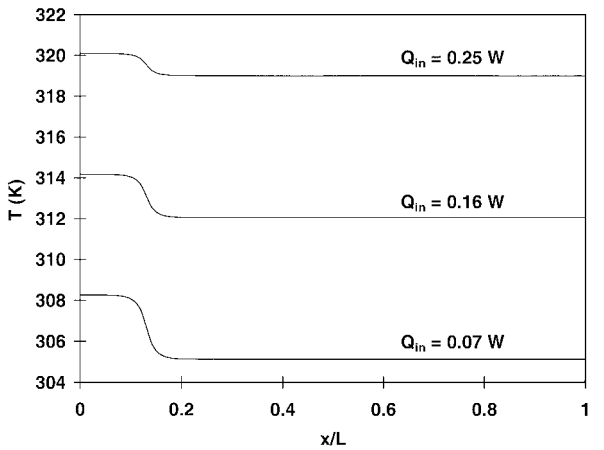

Fig. 5 Steady-state vapor temperature distribution along the micro-heat-pipe channel for various heat inputs at the evaporator.

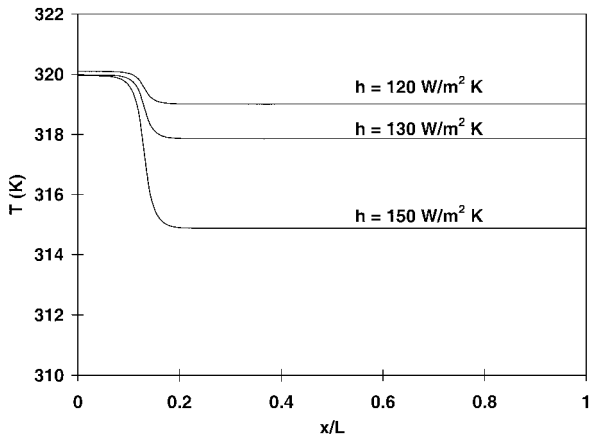

Fig. 6 Steady-state vapor temperature distribution along the channel for a heat input of 0.25 W at the evaporator for various heat transfer coefficients at the condenser section.

of 120 W/m^2 K at the condenser, the drop in the vapor temperature is less than 1 K along the evaporator and condenser sections of the heat pipe, indicating a high effective conductance of the device.

The influence of the input power at the evaporator section on the local vapor temperature is shown in Fig. 5. All of the graphs correspond to steady state, with the same heat transfer coefficient (120 W/m^2 K) applied to the condenser section. At a lower input power value, the temperature dip across the interface between the

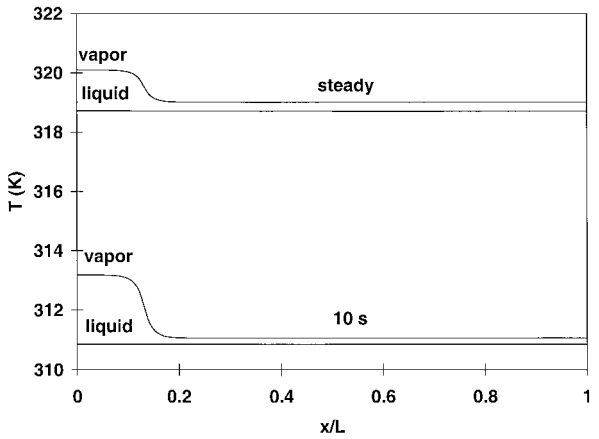

Fig. 7 Comparison of the liquid and vapor temperature distributions at 10 s from the start and at steady state.

evaporator and condenser sections is more than that in the case of a higher heat input. This effect is attributed to the existence of higher velocities in the vapor when higher heat inputs are applied that make the phase change and heat transport processes more efficient, as expected, in the heat pipe. This result indicates that the effective conductance increases with the heat input, when the heat transfer coefficient at the condenser is kept constant. Figure 6 shows the influence of the heat transfer coefficient at the condenser on the vapor temperature distribution, for the same power input at the evaporator.

It is found that the liquid temperature is more or less uniform along the heat pipe. Figure 7 shows a comparison of the vapor and liquid temperatures, at 10 s from the start and at steady state, for the case of 0.25-W input power and a heat transfer coefficient of 120 W/m^2 K at the condenser. The vapor temperature is higher than the liquid temperature everywhere, and this indicates that the vapor is at a superheated state at the evaporator section. Because the liquid portion is confined to the corners of the channel, at the evaporator section, the vapor is directly heated to temperatures higher than that of the liquid. Along the condenser section, the vapor and liquid temperatures are very close to each other.

Transient Variations of Vapor Temperature and Heat Dissipation

The evaporator temperature is the most significant value to be monitored because the evaporator section of the heat pipe is attached to the component to be cooled. The purpose of the heat pipe is to dissipate the heat such that this temperature is kept moderate or as low as possible. The transient variation of the vapor temperature at the evaporator for a typical value of the heat input and convective heat transfer coefficient is shown in Fig. 8. The input heat and the dissipation equalize at steady state. The transient variation of the heat dissipation at the condenser section, from the start until the attainment of steady state, is shown in Fig. 9. This case corresponds to a heat input of 0.25 W at the evaporator and a heat transfer coefficient of 120 Wm^2/K at the condenser. It is seen from the computational results that, for the case presented in Fig. 9, steady state is attained in about 30 s from the start. In the practical case, however, with the influence of the heat pipe material, it is expected that the attainment of steady state would be much slower. This effect has been noticed and discussed in the literature.[5]

Pressure Distribution

The distribution of the liquid and vapor pressure along the micro heat pipe at steady state is shown in Fig. 10. Heat input to the evaporator is 0.25 W, and convective heat transfer coefficient at the condenser is 120 W/m^2 K. The variation of the vapor pressure along the heat pipe is not very significant when compared to that of the liquid. The difference between the vapor and liquid pressures is large in the evaporator section, the liquid pressure being much lower than the pressure of the vapor. The vapor pressure distribution mirrors the vapor temperature distribution. The nature of the vapor pressure

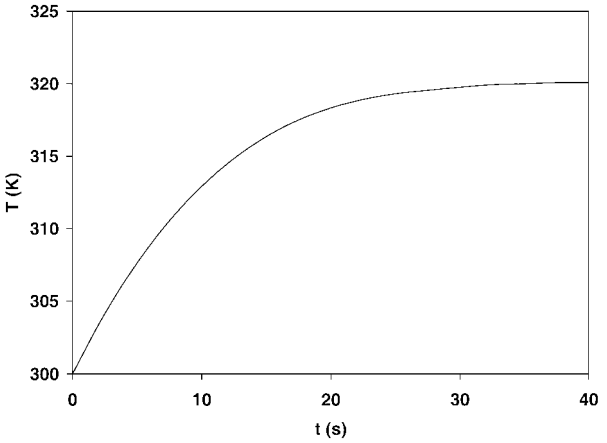

Fig. 8 Transient variation of the vapor temperature at the evaporator for a heat input of 0.25 W at the evaporator and a convective heat transfer coefficient of 120 W/m^2 K at the condenser.

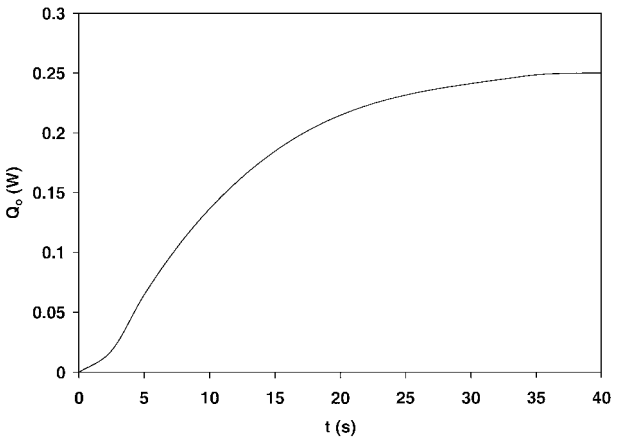

Fig. 9 Transient variation of the heat dissipation at the condenser section.

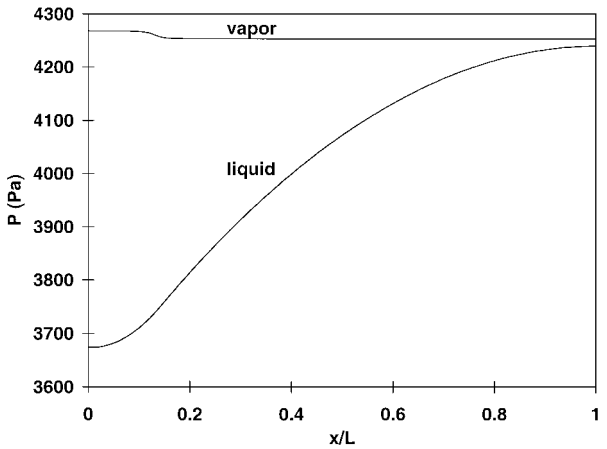

Fig. 10 Vapor and liquid pressure distributions along the micro-heat-pipe channel at steady state.

variation is as expected, due to an almost constant temperature of the vapor along the heat pipe. The variations are in accordance with those discussed in the literature.[5]

Overall Performance of the Micro Heat Pipe

To compare the overall performance of the heat pipe under various operating conditions, a performance parameter, namely, the effective thermal conductivity, has been defined in Eq. (15). This is normalized with respect to the thermal conductivity of copper,

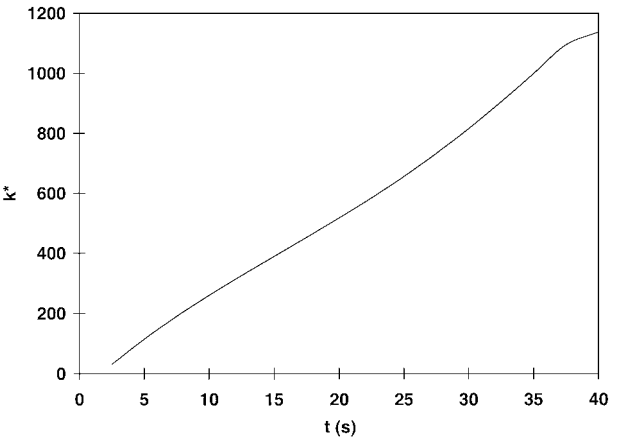

Fig. 11 Transient variation of the instantaneous effective thermal conductivity ratio.

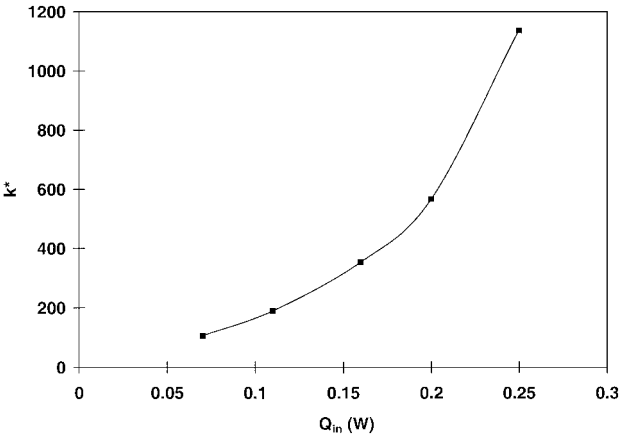

Fig. 12 Dependence of the steady-state effective thermal conductivity ratio on the input power to the evaporator, for a constant heat transfer coefficient at the condenser.

the material of the micro heat pipe. The transient variation of the effective thermal conductivity and the variation of its steady-state value with respect to the heat input to the evaporator section are interesting to study because this parameter gives a picture of the temperature uniformity along the heat pipe in comparison with the heat throughput.

The transient variation of the effective thermal conductivity ratio, for an input power of 0.25 W to the evaporator section of the channel and a convective heat transfer coefficient of 120 W/m^2 K applied to the condenser section, is shown in Fig. 11. In the transient condition, the effective conductivity is calculated based on the heat dissipation from the condenser and not the input power because only a part of the input power is dissipated. The effective conductivity has a transient increase. Figure 12 shows the dependence of the effective thermal conductivity at steady state on the power throughput. All of the cases correspond to a heat transfer coefficient of 120 W/m^2 K at the condenser. There is a significant increase in the value of the effective thermal conductivity with the power throughput, with a constant heat transfer coefficient applied to the condenser. The dependence of the effective thermal conductivity on the power input, for cases where a constant temperature is maintained at the condenser by adjusting the cooling rate, has been presented by Wu et al.[4] and shows a decrease in the value with increasing heat input. The situation is different in the present case from that presented by Ref. 4 because, in the present case, the heat transfer coefficient is kept constant and the temperature is not controlled externally.

Comparison of Results

The vapor temperature drop along the heat pipe obtained through the solution of the energy equation in the present model provides

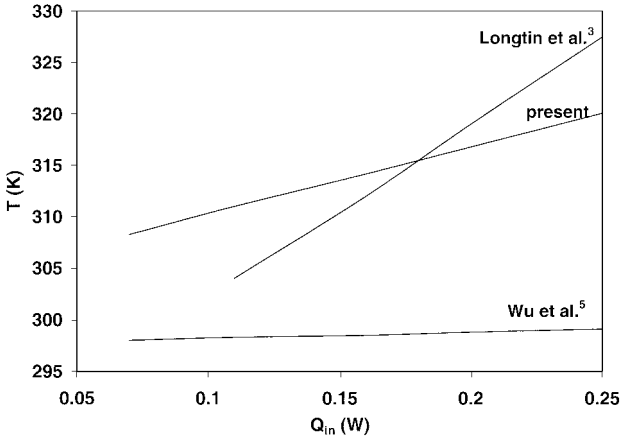

Fig. 13 Comparison of the variation of the vapor temperature at the midpoint of the evaporator section, with respect to the heat input, with results presented in the literature.

a means of calculating a performance parameter for the micro heat pipe, namely, the effective thermal conductivity. This is an advantage of the present model over models that assume a uniform vapor temperature along the heat pipe.

The present model is developed on the same lines as discussed by Longtin et al.[3] but solves the energy equation and extends the solution to the condenser section. The heat pipe analyzed by the authors of Ref. 3 has an extremely small evaporator section of 0.28 mm length, compared to 20 mm length of the adiabatic section. Further, the condenser section is not included in this analysis. Assumption of a uniform vapor temperature along the heat pipe seems to be appropriate in that case. However, it is not justifiable to assume a uniform vapor temperature in the present study because the evaporator length is not of negligible length compared to the total length of the heat pipe. A temperature drop along the heat pipe is expected and is obvious from the calculations.

Even though the physical dimensions and operating conditions differ, a comparison of the present results is made with cases presented by Longtin et al.[3] and Wu et al.[5] Note that the distributions of the field variables and the performance of the micro heat pipe depend on the geometry and the operating conditions such as the surface and cross-sectional areas, the heat input, and the cooling coefficient. However, the comparison presented here would be useful in checking the trend and the orders of magnitude of the quantitative results obtained from the present model.

The dependence of the temperature level of the vapor, indicated by the temperature at the midpoint of the evaporator section, on the applied heat input is shown compared with results presented in literature in Fig. 13. The nature of the variation is linear in all of the cases. The temperatures obtained from the present analysis are greater than those calculated by Wu et al.[5] for the same heat input levels, as expected, due to much smaller peripheral dimensions of the channel and higher heat fluxes associated with the present case. The case reproduced from Wu et al.[5] corresponds to a fixed condenser temperature of 24.5°C, whereas, for the results shown from the present analysis, the heat transfer coefficient and the temperature of the cooling stream at the condenser are fixed at 120 W/m^2 K and 300 K, respectively. The analysis by Longtin et al.[3] is different in that the effects of the vapor and liquid flow velocities and the external cooling of the condenser are not reflected in the vapor temperature because a uniform temperature model is used and the condenser section is not analyzed. Because the cooling conditions at the condenser differ among the three cases presented, the comparisons are mostly of a qualitative nature.

Conclusion

A transient analysis of the vapor and liquid flow in a micro-heat-pipe channel is performed to obtain the distributions of the vapor and liquid velocities, pressures, and temperatures. From the analysis and parametric studies, the following conclusions are drawn.

1) The vapor velocity distributions in the evaporator and condenser sections are linear. The liquid velocity distribution is linear in the evaporator section, but deviates from this nature in the condenser section. This effect is due to the variation in the flow cross-sectional area.

2) A flow reversal is observed near the condenser end at the initial transient period. This is in accordance with what has been observed in the literature. This effect is due to the forcing of liquid from the evaporator region to the condenser region, as a result of lower evaporation rates at the early transient period.

3) The pressure drop in the liquid is larger, compared to that in the vapor. The difference between the liquid and vapor pressures is large in the evaporator section. Toward the end of the condenser section the pressures are almost equal.

4) Most of the temperature fall in the micro heat pipe occurs near the interface between the evaporator and condenser regions. In the condenser region, the temperature is nearly constant.

5) The variations of the effective thermal conductivity of the heat pipe have been studied. The instantaneous effective thermal conductivity increases in the transient period. Also, there is a substantial increase in the effective thermal conductivity with an increase in the heat input at the evaporator, within the operating limits of the micro heat pipe, when the heat transfer coefficient at the condenser is kept constant.

Appendix: Geometric Area Coefficients (Reproduced from Ref . 3)

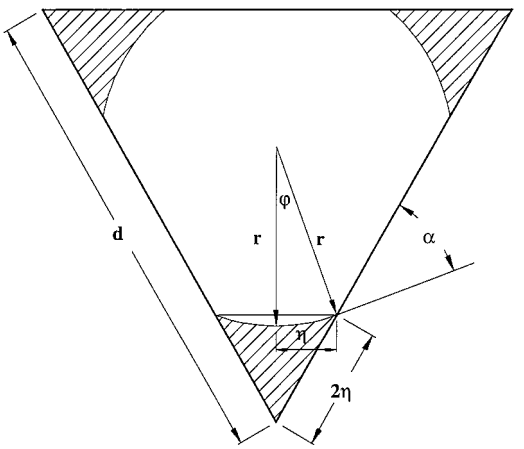

Fig. A1. Cross-sectional geometry for area coefficients.

The cross section is an equilateral triangle with $\varphi = 60 \text{ deg} - \alpha$ and $\eta = r \sin \varphi$ (Fig. A1). The total area of the liquid in the cross section is $A_l = \beta_l r^2$, where

$$\beta_l = 3\left[\sqrt{3}\sin^2(\pi/3 - \alpha) + 0.5 \sin 2(\pi/3 - \alpha) - (\pi/3 - \alpha)\right]$$

The total area of the interface in length dx is $A_i = \beta_i r \, \mathrm{d}x$, where

$$\beta_i = 6(\pi/3 - \alpha)$$

The total wetted perimeter for the three corners $= \beta_{lw} r$, where

$$\beta_{lw} = \pi \sin(\pi/3 - \alpha)$$

Acknowledgment

The authors gratefully acknowledge the support of the National Science and Technology Board, Singapore, for providing Research Grant JT ARC 5/96 under which this investigation was carried out.

References

[1]Babin, B. R., Peterson, G. P., and Wu, D., "Steady State Modeling and Testing of a Micro Heat Pipe," *Journal of Heat Transfer*, Vol. 112, No. 3, 1990, pp. 596–601.

[2]Ma, H. B., and Peterson, G. P., "The Minimum Meniscus Radius and Capillary Heat Transport Limit in Micro Heat Pipes," *Microelectromechanical Systems (MEMS)*, DSC-Vol. 62/HTD Vol. 354, American Society of Mechanical Engineers, Fairfield, NJ, 1997, pp. 213–220.

[3]Longtin, J. P., Badran, B., and Gerner, F. M., "A One Dimensional Model of a Micro Heat Pipe During Steady State Operation," *Journal of Heat Transfer*, Vol. 116, No. 3, 1994, pp. 709–715.

[4]Wu, D., and Peterson, G. P., "Investigation of the Transient Characteristics of a Micro Heat Pipe," *Journal of Thermophysics and Heat Transfer*, Vol. 5, No. 2, 1991, pp. 129–134.

[5]Wu, D., Peterson, G. P., and Chang, W. S., "Transient Experimental Investigation of Micro Heat Pipes," *Journal of Thermophysics and Heat Transfer*, Vol. 5, No. 4, 1991, pp. 539–544.

[6]Khrustalev, D., and Faghri, A., "Thermal Analysis of a Micro Heat Pipe," *Journal of Heat Transfer*, Vol. 116, No. 1, 1994, pp. 189–198.

[7]Peterson, G. P., and Ma, H. B., "Analysis of Counter Current Liquid–Vapor Interactions and the Effect on the Liquid Friction Factor," *Experimental Thermal and Fluid Science*, Vol. 12, No. 1, 1996, pp. 13–24.

[8]Swanson, L. W., and Peterson, G. P., "The Interfacial Thermodynamics of Micro Heat Pipes," *Journal of Heat Transfer*, Vol. 117, No. 1, 1995, pp. 195–201.

[9]Peterson, G. P., Duncan, A. B., Ahmed, A. S., Mallik, A. K., and Weichold, M. H., "Experimental Investigation of Micro Heat Pipes in Silicon Wafers," *Micromechanical Sensors, Actuators and Systems*, DSC-Vol. 32, American Society of Mechanical Engineers, Fairfield, NJ, 1991, pp. 341–348.

[10]Chen, H., Groll, M., and Rosler, S., "Micro Heat Pipes: Experimental Investigation and Theoretical Modelling," *Advances in Heat Pipe Science and Technology: Proceedings of the 8th International Heat Pipe Conference*, International Academic Publishers, Beijing, 1992, pp. 396–400.

[11]Zhou, J., Yao, Z., and Zhu, J., "Experimental Investigation of the Application Characters of Micro Heat Pipe," *Advances in Heat Pipe Science and Technology: Proceedings of the 8th International Heat Pipe Conference*, International Academic Publishers, Beijing, 1992, pp. 421–424.

[12]Zhang, J., Wang, C., Yang, X., and Zhou, Z., "Experimental Investigation of the Heat Transfer Characteristics of the Micro Heat Pipes," *Advances in Heat Pipe Science and Technology: Proceedings of the 8th International Heat Pipe Conference*, International Academic Publishers, Beijing, 1992, pp. 416–420.

[13]Peterson, G. P., "Investigation of Micro Heat Pipes Fabricated as an Integral Part of Silicon Wafers," *Advances in Heat Pipe Science and Technology: Proceedings of the 8th International Heat Pipe Conference*, International Academic Publishers, Beijing, 1992, pp. 385–395.

[14]Cao, Y., Faghri, A., and Mahefkey, E. T., "Micro/Miniature Heat Pipes and Operating Limitations," *Heat Pipes and Capillary Pumped Loops*, ASME HTD-Vol. 236, American Society of Mechanical Engineers, Fairfield, NJ, 1993, pp. 55–62.

[15]Faghri, A., "Recent Advances in the Numerical Analysis of Heat Pipes," *Computational Mechanics*, Vol. 14, No. 5, 1994, pp. 480–491.